Developing turbulent duct flow: hybrid solution via integral transforms and algebraic model

Received August 1994
Revised July 1996

R.M. Cotta and L.C.G. Pimentel
Mechanical Engineering Department, Universidade Federal do Rio de Janeiro, Rio de Janeiro, Brazil

Nomenclature

D_H = hydraulic diameter (= $4r_w$)
N = truncation order of system (10)
N_i = normalization integral, equation (7c)
$\bar{p}, p^*$ = pressure field, dimensional and dimensionless
r, R = transversal co-ordinate, dimensional and dimensionless
r_w = half- distance between parallel-plates
R_e = Reynolds number (= $u_o\, r_w/\upsilon$)
R_c = limit of internal and external boundary layer regions (Appendix 1)
$\bar{u}, \bar{U}$ = longitudinal velocity component, dimensional and dimensionless
u_o = inlet velocity
$U_\infty(R)$ = fully developed velocity distribution
υ,V = transversal velocity component, dimensional and dimensionless
z, Z = longitudinal co-ordinate, dimensional and dimensionless
Z_I = Starting position of intermediate region in the turbulence model (Appendix 1).

Greek Symbols

α = thermal difusivity
ε = relative error in adaptive procedure, equation (13)
ϵ = dimensionless turbulent viscosity
μ_i = eigenvalues of problem (6)
$\Psi_i(R)$ = eigenfunctions of problem (6)
υ = kinematic viscosity
δ = dimensionless boundary layer thickness
ρ = fluid density

Subscripts and Superscripts

- - = integral transformed quantities
i, j, k = order from eigenvalue problem

Introduction

The analysis of turbulent developing duct flow is a crucial step in the proper simulation of heat exchange devices, within various application areas, in the search for an accurate prediction of friction factor and heat transfer coefficients. In opposition to the simpler laminar flow situation, the design procedures are still heavily based on the use of approximate empirical or semi-analytical correlations (Shah and Bhatti, 1987). Besides the inherent difficulties associated with the numerical solution of the associated non-linear boundary layer-type equations, the choice of turbulence model, that completes the problem formulation, is far from unanimous. Both differential and algebraic models compete in the literature on numerical simulation of turbulent duct flows, with specific relative merits in accuracy, simplicity and computational cost (Minkowycz *et al.*, 1988). Among the most frequently referenced turbulence models (Minkowycz *et al.*, 1988), the local algebraic model of Cebeci and Smith (1974) is very well accepted in the analysis of internal flows, in light of the good

International Journal for Numerical Methods for Heat & Fluid Flow
Vol. 8 No. 1, 1998, pp. 10–26.

agreement achieved against experimental results for the velocity distributions (Cebeci and Chang, 1978), in both circular tube and parallel-plates geometries.

Without exception, the available turbulence models require some sort of adjustment in order to roughly match experimental measurements, through certain coefficients pertinent to the specific model considered. Therefore, it would be quite desirable to devise a fully error-controlled numerical procedure for the turbulent boundary layer equations, not to contaminate the adjusted coefficients with non-converged numerical results, and allow for an improved matching of theoretical and experimental findings. Quite recently, based on the ideas of the so-called generalized integral transform technique (Cotta, 1993), hybrid numerical-analytical solutions with automatic global error control were obtained, for different classes of non-linear heat and fluid flow problems (Boohua and Cotta, 1993; Campos Silva *et al.*, 1992; Carvalho *et al.*, 1993; Cotta, 1990; Cotta and Carvalho, 1991; Cotta and Serfaty, 1991; Cotta *et al.*, 1992; Diniz *et al.*, 1990; Leiroz and Cotta, 1993; Machado and Cotta, 1995; Pérez Guerrero and Cotta, 1992; Pérez Guerrero *et al.*, 1993; Serfaty and Cotta, 1990; Serfaty and Cotta, 1992), including the laminar boundary layer equations for duct flow (Campos Silva *et al.*, 1992; Carvalho *et al.*, 1993; Cotta and Carvalho, 1991; Machado and Cotta, 1995).

Within this context, the present work further advances the integral transform approach by handling the boundary layer equations for developing duct flow in the turbulent regime. The Cebeci-Smith algebraic model is chosen to provide the required equations for the turbulent diffusivity, allowing for the illustration of the proposed procedure. The convergence behavior of the eigenfunction expansions is demonstrated and different choices of eigenvalue problem are discussed. Fully converged numerical results for the velocity components are then critically compared with experimental results, as well as against numerical results from previous works that employed different turbulence models.

Analysis

We consider incompressible turbulent flow of a Newtonian fluid, developing between parallel plates from the duct entrance with a uniform inlet velocity distribution. Within the range of validity for the turbulent boundary layer formulation, the flow problem is written, in dimensionless form, as:

– Continuity

$$\frac{\partial U(R,Z)}{\partial Z}+\frac{\partial V(R,Z)}{\partial R}=0, \quad 0<R<1, Z>0 \tag{1a}$$

– Z-momentum equation:

$$U\frac{\partial U}{\partial Z}+V\frac{\partial U}{\partial R}=-\frac{dp^*}{dZ}+\frac{1}{Re}\frac{\partial}{\partial R}\left[(1+\epsilon)\frac{\partial U}{\partial R}\right], \quad 0<R<1, \quad Z>0 \tag{1b}$$

with inlet and boundary conditions given respectively by

$$U(R,0) = 1; \qquad V(R,0) = 0 \tag{1.c,d}$$

$$\left.\frac{\partial U}{\partial R}\right|_{R=0} = 0; \qquad V(0,Z) = 0 \tag{1.e,f}$$

$$U(1,Z) = 0; \qquad V(1,Z) = 0 \tag{1.g,h}$$

where various dimensionless groups are defined as

$$Z = \frac{z}{r_w}; \quad R = \frac{r}{r_w}; \quad U = \frac{\bar{u}}{u_o}; \quad V = \frac{\bar{v}}{u_o} \; p^* = \frac{\bar{p}}{\rho u_o^2}; \quad Re = \frac{u_o r_w}{\nu}; \quad \epsilon = \frac{\nu_t}{\nu} \tag{2}$$

The algebraic turbulence model employed (Cebeci and Chang, 1978; Cebeci and Smith, 1974) is briefly described in Appendix 1, which provides the required expressions for the turbulent diffusivity in dimensionless form, ϵ.

For improved convergence behavior in the eigenfunction expansions, the fully developed flow solution, $U_\infty(R)$, is filtered from the above equations, in the form:

$$U(R,Z) = U^*(R,Z) + U_\infty(R) \tag{3}$$

where the expression for $U_\infty(R)$ is presented in Appendix 2.

After substitution of equation (3) into the original equations (1), the problem formulation becomes:

$$\frac{\partial U^*(R,Z)}{\partial Z} + \frac{\partial V(R,Z)}{\partial R} = 0, \tag{4a}$$

$$(U^* + U_\infty)\frac{\partial U^*}{\partial Z} + V\left(\frac{\partial U^*}{\partial R} + \frac{dU_\infty}{dR}\right) = -\frac{dp^*}{dZ} + \frac{1}{Re}\frac{\partial}{\partial R}\left[(1+\epsilon)\frac{\partial U^*}{\partial R}\right] + \frac{1}{Re}\frac{\partial}{\partial R}\left[(1+\epsilon)\frac{dU_\infty}{dR}\right] \tag{4b}$$

with the modified inlet condition

$$U^*(R,0) = 1 - U_\infty(R) \tag{4c}$$

while the remaining conditions are kept unaltered.

We proceed by eliminating the dependent variables V and p^* from the momentum equation (4b) to be solved for the longitudinal velocity component, U^*.

Therefore, from direct integration of the continuity equation (4a), one finds:

$$V(R,Z) = \int_R \frac{\partial U^*(R',Z)}{\partial Z} dR' \tag{5a}$$

while the dimensionless pressure gradient is obtained from integration of the momentum equation over the channel cross-section to yield

$$-\frac{dp^*}{dZ} = 2\int_0^1 \left[U^* + U_m\right]\frac{\partial U^*}{\partial Z} dR - \frac{1}{Re}\left[\frac{\partial U^*}{\partial R}\Big|_{R=1} + \frac{dU_m}{dR}\Big|_{R=1}\right] \tag{5b}$$

Following the ideas in the generalized integral transform technique (Cotta, 1993), an auxiliary problem is selected to provide a basis for the eigenfunction expansion. One possible choice is given by:

$$\frac{d^2\psi_i(R)}{dR^2} + \mu_i^2\psi_i(R) = 0, \quad 0 < R < 1 \tag{6a}$$

$$\frac{d\psi_i}{dR}\Big|_{R=0} = 0; \qquad \psi_i(1) = 0 \tag{6b,c}$$

which is readily solved to yield

$$\mu_i = \frac{(2i-1)}{2}\pi; \qquad \psi_i(R) = \cos\mu_i R \tag{7a,b}$$

and the normalization integral becomes

$$Ni = \int_0^1 \psi_i^2(R)\, dR = \frac{1}{2} \tag{7c}$$

A second possible choice of eigenvalue problem, which incorporates some information on the turbulent diffusivity profile, is discussed later.

Problem (6) above allows definition of the following integral transform pair

$$\overline{U}_i^*(Z) = \frac{1}{N_i^{1/2}}\int_0^1 \psi_i(R)U^*(R,Z)dR, \quad \text{transform} \tag{8a}$$

$$U^*(R,Z) = \sum_{i=1}^{\infty}\frac{1}{N_i^{1/2}}\psi_i(R)\overline{U}_i^*(Z), \qquad \text{inversion} \tag{8b}$$

The transversal velocity component and the pressure gradient may be expressed in terms of the transformed potential, $\overline{U}_i^*(Z)$ as:

$$V(R,Z) = \sum_{j=1}^{\infty} F_j(R)\frac{d\overline{U}_k^*}{dZ} \tag{9a}$$

$$-\frac{dp^*}{dZ} = 2\sum_{k=1}^{\infty}\bar{U}_k^*(Z)\frac{d\bar{U}_k^*}{dZ} + z\sum_{k=1}^{\infty}H_k\frac{d\bar{U}}{dZ} - \frac{1}{Re}\left\{\sum_{k=1}^{\infty}\frac{\psi_k'(1)}{N_k^{1/2}}\bar{U}_k^* + \frac{dU_\infty}{dR}\Big|_{R=1}\right\} \quad (9b)$$

where

$$F_j(R) = \frac{1}{N_j^{1/2}}\int_R \psi_j(R')dR' \quad (9c)$$

$$H_k = \frac{1}{N_k^{1/2}}\int_0 \psi_k(R)U_\infty(R)dR \quad (9d)$$

The integral transformation process in now performed, by applying the operator

$$\frac{1}{N_i^{1/2}}\int_0 \psi_i(R)dR$$

on equation (4b); after substitution of expressions (9a,b) above, the following ordinary differential system results

$$\sum_{k=1}^{\infty}\left\{\sum_{j=1}^{\infty}\left[A_{ijk} + B_{ijk} - 2F_i(0)\delta_{jk}\right]\bar{U}_j^* + Q_{ik} + S_{ik} - 2F_i(0)H_k\right\}\frac{d\bar{U}_k^*}{dZ} =$$

$$-\frac{1}{Re}\left[\sum_{k=1}^{\infty}\left(F_i(0)\frac{\psi_k'(1)}{N_k^{1/2}} + \delta_{ik}\mu_k^2 + M_{ik}\right)\bar{U}_k^* + \frac{dU_\infty}{dR}\Big|_{r=1} + Z_i\right], \qquad i = 1,2,\ldots \quad (10a)$$

and the inlet condition (4.c) is similarly transformed to yield

$$\bar{U}_i^*(0) = \bar{f}_i = \frac{1}{N_i^{1/2}}\int_0 \psi_i(R)\left[1 - U_\infty(R)\right]dR \quad (10b)$$

where the various coefficients are given by

$$A_{ijk} = \frac{1}{N_i^{1/2}N_j^{1/2}N_k^{1/2}}\int_0 \psi_i(R)\psi_j(R)\psi_k(R)dR \quad (11a)$$

$$B_{ijk} = \frac{1}{N_i^{1/2}N_j^{1/2}}\int_0 \psi_i(R)\psi_j'(R)F_k(R)dR \quad (11b)$$

$$Q_{ik} = \frac{1}{N_i^{1/2}N_k^{1/2}}\int_0 \psi_i(R)\psi_k(R)U_\infty(R)dR \quad (11c)$$

$$S_{ik} = \frac{1}{N_i^{1/2}} \int_0^1 \psi_i(R) F_k(R) \frac{dU_\infty}{dR} dR \tag{11d}$$

$$M_{ik} = \frac{1}{N_i^{1/2} N_k^{1/2}} \int_0^1 \psi_i'(R) \psi_k'(R) \in (R,Z) dR \tag{11e}$$

$$Z_i = \frac{1}{N_i^{1/2}} \int_0^1 \psi_i'(R) [1 + \in (R,Z)] \frac{dU_\infty}{dR} dR \tag{11f}$$

$$\delta_{jk} = \begin{cases} 0, & i \neq k \\ 1, & i = k \end{cases} \tag{11g}$$

Some of the integrals above are readily evaluated in analytic form, while those depending on the turbulent diffusivity (or on the transformed potential itself) are evaluated numerically through subroutines with automatic schemes for error control (IMSL Library, 1987). For computational purposes, the infinite system (10) is truncated to a sufficiently large order so as to satisfy the user prescribed accuracy requirements. In fact, this truncation order is automatically selected and varied along the course of integration of system (10), as described in the next section. The non-linear ODE system is also handled through scientific subroutine libraries with well-tested error control schemes (IMSL Library, 1987).

Once the transformed potentials, $\bar{U}_k^*$, have been numerically obtained at any position Z of interest, the original longitudinal velocity component is determined from:

$$U(R,Z) = U_\infty(R) + \sum_{i=1}^{N} \frac{1}{N_i^{1/2}} \psi_i(R) \bar{U}_i^*(Z) \tag{12}$$

Computational procedure

The computations are implemented through the use of well-established subroutines for numerical integration and solution of implicit stiff ODE systems, such as those available in IMSL Library (1987). These routines incorporate automatic relative error control schemes, which allow for conservative evaluations towards a user requested accuracy. Since all the intermediate numerical tasks are accomplished within user prescribed accuracy, one is left with the need to control the global solution error, through the convergence analysis of the eigenfunction expansion. Therefore, in order to implement an automatic procedure, the truncation order, N, must be chosen adaptively during the course of computation, for a certain number of fully converged digits requested in the final solution, at those positions of interest.

The analytic nature of the inversion formula allows for a direct testing scheme at each specified position where a solution is required, and the truncation order, N, can be gradually varied, either reduced or increased when needed, to meet the user error requirements. The simple formula for checking the accuracy achieved is given by:

$$\varepsilon = \max_{0 \le R \le 1} \left| \frac{\sum_{i=N^*}^{N} \frac{\psi_i(R)}{N_i^{1/2}} \bar{U}_i^*(Z)}{U_\infty(R) + \sum_{i=1}^{N} \frac{\psi_i(R)}{N_i^{1/2}} \bar{U}_i^*(Z)} \right| \tag{13}$$

where N^* is reduced with respect to N while ε still fits the user requested precision; at this limit, N is changed to assume the value of N^*, and the integration proceeds to the next requested value of Z, with a reduced number of ODEs. The truncation order can also be increased and the integration from the previous value of Z be repeated, in case convergence was not achieved. At each desired Z, a fully converged solution will then be available, at the desired precision, together with the error estimation itself, and reducing computational costs.

Results and discussion

The computational procedure was implemented on a VAX8810 mainframe computer, with a global prescribed relative error of 10^{-4}, i.e. the final converged results are expected to be accurate to ± 1 in the fourth digit provided. Truncation orders of $N \le 25$ were required to achieve convergence, along a wide range of the dimensionless longitudinal co-ordinate.

Numerical results were obtained for different values of the Reynolds number, and compared critically against experimental and previously reported numerical results. First, the convergence rates of the eigenfunction expansion are illustrated, at different positions along the duct length, $Z/_{DHH}$ = 10 and 25, for Re = 4.8×10^4. Tables I and II show the longitudinal velocity profiles at these

Table I.
Convergence of the longitudinal velocity profile

	Nc					
R	5	9	13	17	21	25
0.0	1.134	1.143	1.102	1.101	1.100	1.100
0.2	1.125	1.136	1.101	1.001	1.100	1.100
0.4	1.105	1.122	1.089	1.089	1.088	1.088
0.6	1.057	1.077	1.045	1.044	1.046	1.046
0.8	0.9530	0.9676	0.9146	0.9147	0.9143	0.9143
0.9	0.8553	0.8620	0.8229	0.8227	0.8227	0.8228

R	Nc 5	9	13	17	21	25
0.0	1.137	1.139	1.144	1.143	1.142	1.142
0.2	1.116	1.118	1.123	1.122	1.121	1.121
0.4	1.076	1.077	1.080	1.080	1.079	1.080
0.6	1.017	1.017	1.019	1.019	1.018	1.018
0.8	0.9238	0.9237	0.9244	0.9244	0.9242	0.9243
0.9	0.8387	0.8387	0.8390	0.8390	0.8390	0.8390
0.94	0.7789	0.7788	0.7790	0.7790	0.7798	0.7798
0.98	0.6457	0.6457	0.6460	0.6458	0.6479	0.6479

Table II.
Convergence of the longitudinal velocity profile

positions respectively. For the position closer to the duct inlet, as usual in eigenfunction expansions approaches, a larger number of terms is required, and full convergence to four digits is achieved with $N \leq 21$, while at $^{Z}/_{D_H} = 25$ the convergence rate is clearly improved. The columns for $N = 25$ provide a set of benchmark results for the velocity distribution. This trend is also presented in graphical form, through Figures 1 and 2. On the graph scale, the results for $^{Z}/_{D_H}$

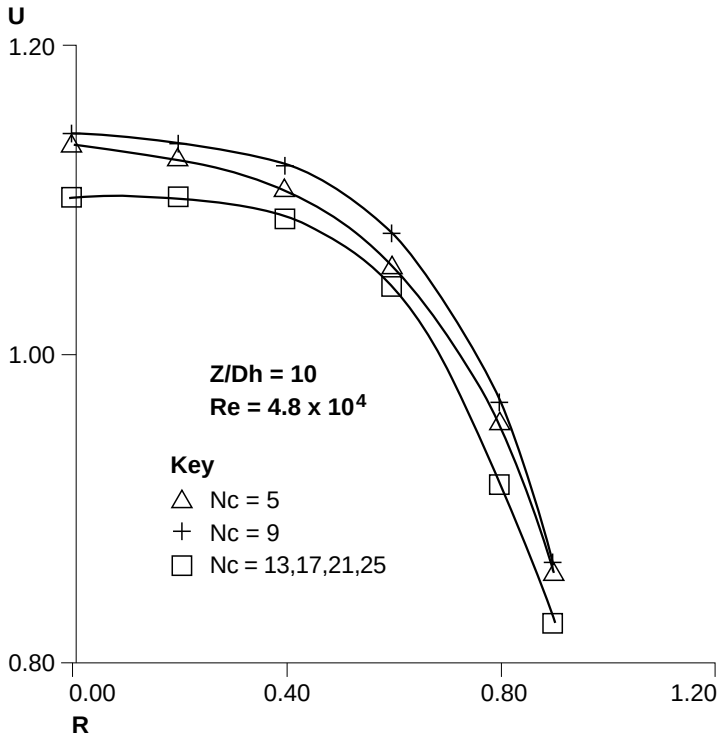

Figure 1.
Convergence of longitudinal velocity profile ($Re = 4.8 \times 10^4$; $^{Z}/_{D_H} = 10$)

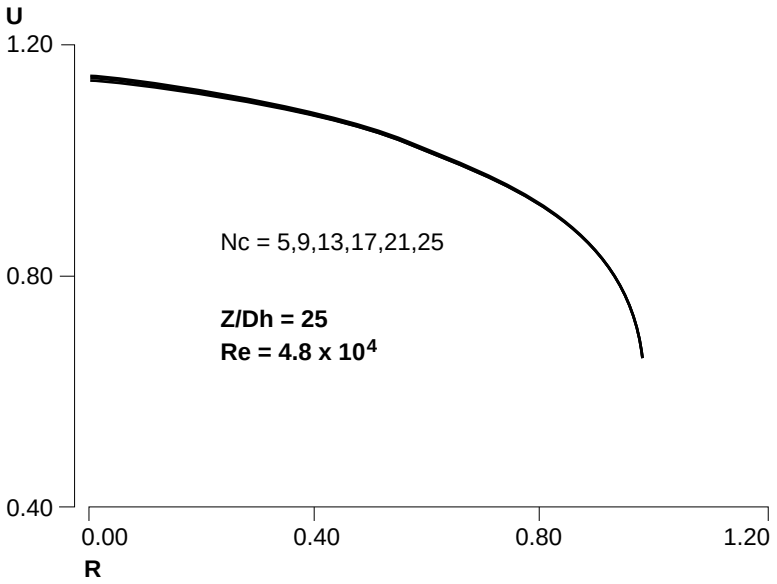

Figure 2.
Convergence of longitudinal velocity profile ($Re = 4.8 \times 10^4$; $^{Z}/_{D_H} = 25$)

= 10 are practically coincident for $N \geq 13$, while for $^{Z}/_{D_H} = 25$, N as low as five already presents a very good agreement with the fully converged results. Also of interest is the illustration of the convergence behavior for the centerline velocity along the whole channel length. Table III and Figure 3 show the centerline velocity along $^{Z}/_{D_H}$, for $Re = 4.8 \times 10^4$, as computed from different truncation orders. Again quite noticeable is the improvement on convergence rates for increasing dimensionless duct length, with full convergence to four digits achieved, in the worst situation, for $N \leq 21$. From Figure 3, it can be seen that within the intermediate region of the turbulence model, convergence of the

	Nc					
R	5	9	13	17	21	25
5	1.069	1.066	1.038	1.036	1.034	1.034
10	1.136	1.143	1.101	1.100	1.100	1.100
15	1.149	1.153	1.162	1.142	1.152	1.152
20	1.146	1.149	1.156	1.154	1.152	1.152
25	1.137	1.139	1.144	1.143	1.142	1.142
30	1.131	1.132	1.135	1.135	1.134	1.134
35	1.126	1.127	1.129	1.129	1.129	1.129
40	1.124	1.124	1.125	1.125	1.125	1.125
45	1.122	1.122	1.123	1.123	1.123	1.123
50	1.121	1.121	1.122	1.122	1.122	1.122

Table III.
Convergence of the longitudinal centerline velocity

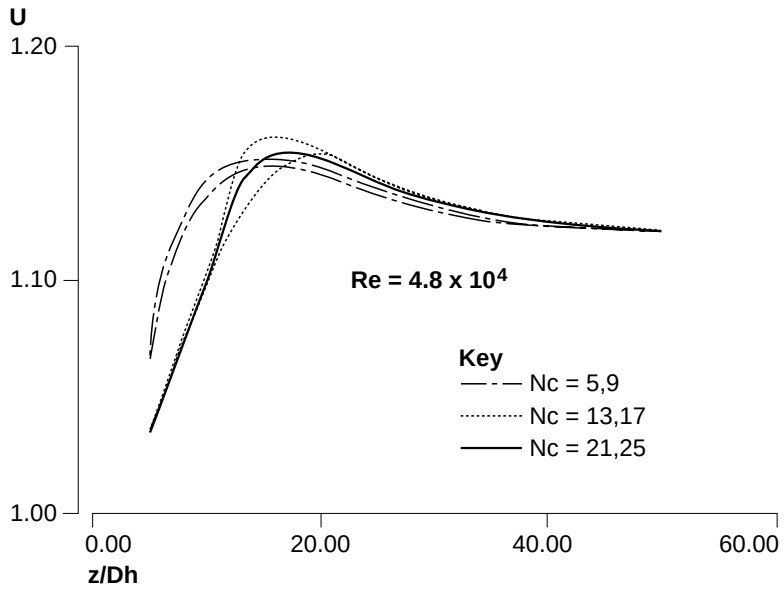

Figure 3.
Convergence of centerline velocity along channel length ($Re = 4.8 \times 10^4$)

velocity field is not achieved until all the parameters involved in the model are also converged, including the starting position of the intermediate region, Z_I, which occurs for $N \cong 13$.

Figure 4 illustrates the automatic control of the truncation order, N, along the integration path in the Z co-ordinate, for different values of Re = 3.5×10^4, 4.8×10^4, 5.0×10^4, and 1.0×10^5. A slight influence of the Reynolds number

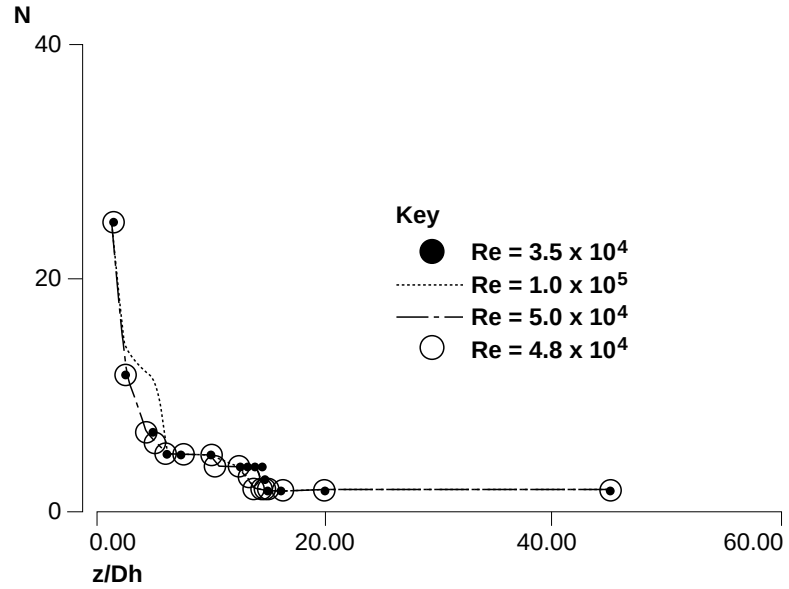

Figure 4.
Automatic control of truncation orders in the eigenfunction expansions, for different Reynolds numbers

on convergence rates is observed from the behavior for the larger value of $Re = 1.0 \times 10^5$. This adaptive procedure of controlling the order of the eigenfunction expansions, and consequently the size of the truncated ODE system for the transformed potentials, results in a marked reduction of the computation cost and offers a continuous error estimation scheme at any desired position within the solution domain.

Figures 5 and 6 present a comparison among the integral transform results, the experimental analysis of Dean (1972), and the finite differences results of

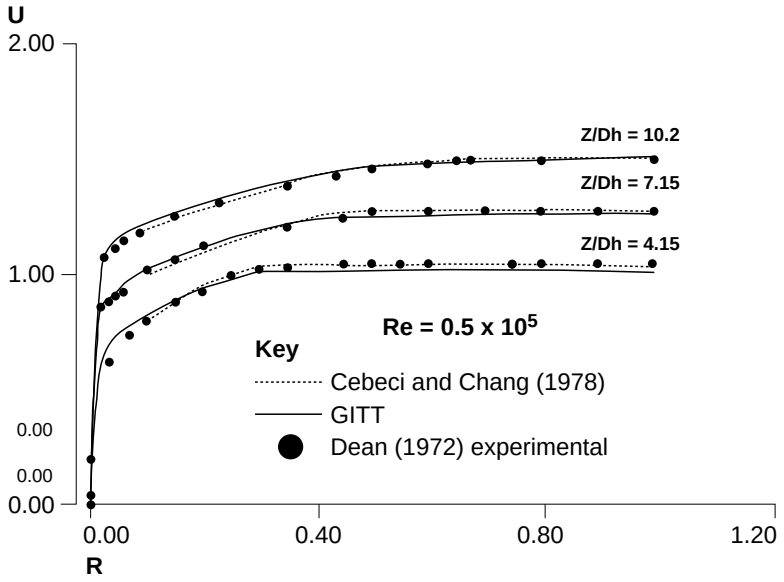

Figure 5.
Comparison of theoretical and experimental results for the longitudinal velocity profile ($Re = 0.5 \times 10^5$)

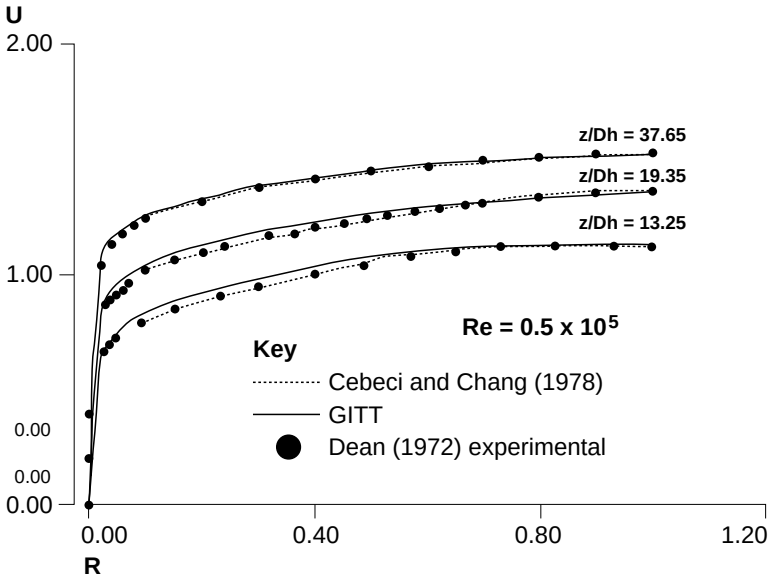

Figure 6.
Comparison of theoretical and experimental results for the longitudinal velocity profile ($Re = 0.5 \times 10^5$)

Cebeci and Chang (1978), that employed essentially the same turbulence model. The value of Re = 0.5×10^5 was employed in these comparisons, and the longitudinal velocity profiles are shown for different axial distances, z/D_H = 4.15, 7.15, 10.2, 13.25, 19.35 and 37.65. The overall agreement is quite good, with a maximum deviation of the two theoretical approaches of about 4 per cent between themselves, and an even better agreement with the experimental results. A similar comparison is presented in Figure 7, where the integral transform results are again compared against experimental results due to Byrne *et al.* (1969) and previously reported numerical results obtained by Zaparoli (1989), where a differential k-ε turbulence model was employed. The value of Re = 3.5×10^4 is chosen in this set of results, and different values of z/D_H = 10, 20 and 30. Again, the agreement among the three sets of results is quite good, with relative deviations below 4 per cent.

Figure 8 brings an interesting comparison related to the evolution of the centerline velocity along the channel, for Re = 4.8×10^4, including the present results, the numerical results of Cebeci and Chang (1978), the finite differences/ $k - \in$ model results of Zaparoli (1989) and the experimental results of Dean (1972). Clearly, the best agreement with the experiments is achieved by the simulation of Cebeci and Chang (1978), followed by the integral transform solution, with a noticeable deviation in the location of the maximum centerline velocity. However, it should be remembered that this situation was adjusted to match experimental and theoretical results (Cebeci and Chang, 1978), through the parameter λ in the intermediate region, according to the analysis of Cebeci and Chang (1978). The question is then raised whether the adopted value of λ = 20 could be contaminated with the numerical uncertainties of the computational scheme itself. Some preliminary numerical experiments demonstrated that some variation on the value of λ (for instance, λ = 30), could

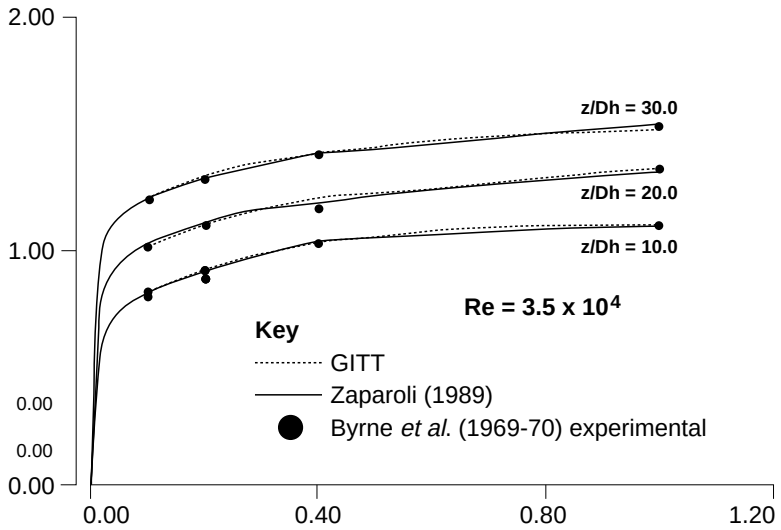

Figure 7. Comparison of theoretical and experimental results for the longitudinal velocity profile (Re = 3.5×10^4)

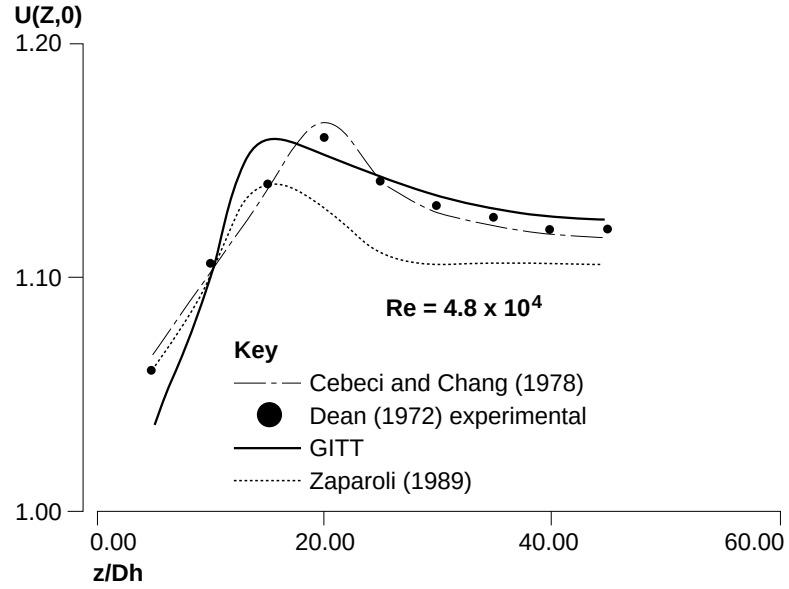

Figure 8.
Comparison of theoretical and experimental results for the centerline velocity evolution ($Re = 4.8 \times 10^4$)

offer an improved agreement of the present results, with user-prescribed accuracy, and the experimental results of Dean (1972). Additional study is then required for the establishment of a more definitive recommended value of this important parameter. Nevertheless, the present results deviate from the analysis of Cebeci and Chang (1978) by a maximum of about 3 per cent along the whole solution domain.

Meanwhile, Figure 9 shows the evolution of the centerline velocity, as obtained through the integral transform approach, for different values of the

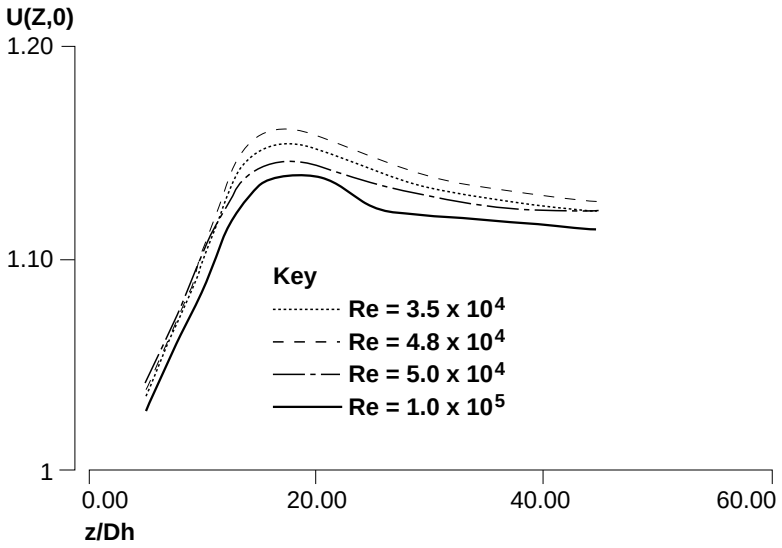

Figure 9.
Evolution of the centerline velocity along channel length for different Reynolds numbers

Reynolds number, Re = 3.5×10^4, 4.8×10^4, 5.0×10^4 and 1.0×10^5. The expected physical trends are clearly observable from this figure, in all cases indicating that the maximum centerline velocity position is located before the fully developed region, as opposed to the laminar flow situation. Also, the increase in Reynolds number promotes the expected decrease of the centerline velocity levels.

A second choice of eigenvalue problem was also considered, which incorporates in its diffusion operator the information on the fully developed turbulent diffusivity, $\epsilon_\infty(R)$. An explicit straightforward solution to the auxiliary problem is then not achievable, but the integral transform method itself (Cotta, 1993; Mikhailov and Cotta, 1994) was employed in the accurate solution for eigenvalues and related eigenfunctions. The fully converged results from this alternative eigenfunction expansion are in perfect agreement with those obtained through the present basis, represented by problem (b). As expected, there was an improvement on convergence rates, especially for regions not so close to the duct inlet, but on overall computational performance, the present proposition still offers advantages in simplicity and costs in terms of CPU time.

The generalized integral transform technique (Cotta, 1993) has proved to be a feasible approach in the analysis of developing duct flows, both for laminar and turbulent regimen, providing a hybrid numerical-analytical solution of the velocity components, with the attractive feature of automatic global error control. This aspect might offer advantages over purely numerical approaches, in the calibration of turbulence models against experimental results, through a more precise adjustment of the pertinent coefficients. Also, the present progress will allow for the extension towards the consideration of more involved differential turbulence models, following this trend in the most of the literature.

References

Arpaci, V.S. and Larsen, P.S. (1984), *Convection Heat Transfer*, Prentice-Hall, London.

Baohua, C. and Cotta, R.M. (1993), "Integral transform analysis of natural convection in porous enclosures", *Int. J. Num. Meth. Fluids*, Vol. 17, pp. 787-801.

Bradshaw, P., Cebeci, T. and Whitelaw, J.H. (1981), *Engineering Calculation Methods for Turbulent Flows*, Academic Press, London.

Byrne, J., Hatton, A.P. and Marriot, P.G. (1969-70), "Turbulent flow and heat transfer in entrance region of parallel wall passage", *Proceedings, Inst. Mech. Eng.*, Vol. 184, part. 1, No 39, p. 697.

Campos Silva, J.B., Cotta, R.M. and Aparecido, J.B. (1992), "Analytical solution to simultaneously developing laminar flow inside parallel-plates channel", *Int. J. Heat & Mass Transfer*, Vol. 35, pp. 887-95.

Carvalho, T.M.B., Cotta, R.M. and Mikhailov, M.D. (1993), "Flow development in the entrance region of ducts", *Comm. Num. Meth. Eng.*, Vol. 9, pp. 503-09.

Cebeci, T. and Chang, K.C. (1978), "A general method for calculating momentum and heat transfer in Laminar and turbulent duct flows", *Num. Heat Transfer*, Vol. 1, pp. 39-68.

Cebeci, T. and Smith, A.M.O. (1974), *Analysis of Turbulent Boundary Layers*, Academic Press, New York, NY.

Cotta, R.M. (1990), "Hybrid numerical-analytical approach to nonlinear diffusion problems", *Num. Heat Transfer, part B – Fundamentals*, Vol. 17, pp. 217-26.

Cotta, R.M. (1993), *Integral Transforms in Computational Heat and Fluid Flow*, CRC Press, Boca Raton, FL.

Cotta, R.M. and Carvalho, T.M.B. (1991), "Hybrid analysis of boundary layer equations for internal flow problems", *7th Int. Conf. on Num. Meth. for Thermal Problems*, Part I, July, pp. 106-15, Stanford, CA.

Cotta, R.M. and Serfaty, R. (1991), "Integral transform algorithm for parabolic diffusion problems with nonlinear boundary and equation source terms", *7th Int. Conf. on Num. Meth. for Thermal Problems, Part II*, July, pp. 916-26, Stanford, CA.

Cotta, R.M., Pérez Guerrero, J.S. and Scofano Neto, F. (1992), "Hybrid solution of the incompressible Navier-Stokes equations via integral transformation", *2nd Int. Conf. Adv. Comp. Meth. in Heat Transfer*, Vol. 1, pp. 735-50, Milan.

Dean, R.B. (1972), "Interaction of turbulent shear layers in duct flow", PhD dissertation, London University.

Diniz, A.J., Aparecido, J.B. and Cotta, R.M. (1990), "Heat conduction with ablation in a finite slab", *Int. J. Heat & Tech.*, Vol. 8, pp. 30-43.

IMSL Library (1987), MATH/LIB, Houston, TX.

Leiroz, A.J.K. and Cotta, R.M. (1993), "On the solution of nonlinear elliptic convection-diffusion problems through the integral transform method", *Num. Heat Transfer, part B-Fundamentals*, Vol. 23, pp. 401-11.

Machado, H.A. and Cotta, R.M. (1995), "Integral transform method for boundary layer equations in simultaneous heat and fluid flow problems", *Int. J. Num. Meth. Heat & Fluid Flow*, Vol. 5, pp. 225-37.

Mikhailov, M.D. and Cotta, R.M. (1994), "Integral transform method for eigenvalue problems", *Comm. Num. Meth. Eng.*, Vol. 10, pp. 827-35.

Minkowycz, W.J., Sparrow, E.M., Schneider, G.E. and Pletcher, R.H. (Eds) (1988), *Handbook of Numerical Heat Transfer*, John Wiley, New York, NY.

Perez Guerrero, J.S. and Cotta, R.M. (1992), "Integral transform method for the Navier-Stokes equations in streamfunction-only formulation", *Int. J. Num. Meth. Fluids*, Vol. 15, pp. 399-409.

Pérez Guerrero, J.S., Cotta, R.M. and Scofano Neto, F. (1993), "Integral transformation of Navier-Stokes equations for incompressible laminar flow in channels", *8th Int. Conf. Num. Meth. in Laminar & Turbulent Flow*, Vol. 2, pp. 1195-1206, Swansea.

Serfaty, R. and Cotta, R.M. (1990), "Integral transform solutions of diffusion problems with nonlinear equation coefficients", *Int. Comm. Heat & Mass Transfer*, Vol. 17, pp. 851-67.

Serfaty, R. and Cotta, R.M. (1992), "Hybrid analysis of transient nonlinear convection-diffusion problems", *Int. J. Num. Meth. Heat & Fluid Flow*, Vol. 2, pp. 55-62.

Shah, R.K. and Bhatti, M.S. (1987), "Turbulent convective heat transfer in ducts", in Kakaç, S., Shak, R.K. and Aung, W. (Eds), *Handbook of Single-Phase Convective Heat Transfer*, John Wiley, New York, NY.

Zaparoli, E.L. (1989), "Calculation of turbulent flow and heat transfer in the entry region of tubes and parallel-plates with two versions of the k-e model for low Reynolds numbers", DSc dissertation (in Portuguese), Instituto Tecnológico de Aeronáutica, São Paulo.

Appendix 1. Turbulence model (Bradshaw *et al.*, 1981; Cebeci and Chang, 1978; Cebeci and Smith, 1974; Mikhailov *et al.*, 1988)

The Cebeci-Smith model describes the turbulent viscosity along the flow direction, for three distinct regions, namely, inlet, intermediate, and fully developed flow regions. The expressions here employed are now summarized for each individual flow region.

Inlet region ($O<Z<Z_I$)

This region is characterized by a weak interaction of the boundary layers, and is then subdivided into an internal region, where inertia terms are neglected, and the external region, where viscous

effects are not relevant. The respective relations for the dimensionless turbulent viscosity are given by:

- Internal boundary layer region ($R_c<R<1$)

$$\epsilon_{IN} = Re\left\{0.4(1-R)\left[1-\exp\left(\frac{R_w}{A}(R-1)\right)\right]\right\}^2\left|\frac{\partial U}{\partial R}\right| \tag{A1}$$

where,

$$\frac{R_w}{A} = \frac{1}{26}\left(-R_c\left.\frac{\partial U}{\partial R}\right|_{R=1}\right)^{1/2} \tag{A2}$$

and the boundary layer thickness, δ, is defined as the transversal length for which the longitudinal velocity component reaches 99.9 per cent of its centerline value, or

$$U((1-\delta), Z) = 0.999\ U(0,Z) \tag{A3}$$

The criteria adopted here might differ from that utilized in Cebeci and Chang (1978), which is not clearly pointed out.

- External boundary layer region ($0 < R < R_c$)

$$\epsilon_{ex} = 0.0168\,Re\left|\int_0^1 [U(0,Z) - U(R,Z)dR]\right| \tag{A4}$$

where the limit between the internal and external regions, R_c, is determined by matching the diffusivities in the two sub-regions

$$\epsilon_{IN}(R_c, Z) = \epsilon_{EX}(Z) \tag{A5}$$

Intermediate region ($Z_I<Z<Z_H$)

This region involves complex interactions and the model needs to be adjusted against experimental results. The inlet region model is employed until a Z position in which the boundary layer thickness reaches 95 per cent of half the distance between the parallel-plates, which defines the initial position of the intermediate region, Z_I. From this point on, the turbulent viscosity profile obtained through the inlet region model is utilized in conjunction with the fully developed region profile, according to the following expression:

$$\epsilon_1 = \epsilon_0(Z_1,R) + [\epsilon_\infty - \epsilon_0(Z_1,R)]\left[1-\exp\left(\frac{Z_1 - Z}{\lambda}\right)\right] \tag{A6}$$

where $\epsilon_0(Z_I,R)$ is the turbulent viscosity at $Z = Z_I$ obtained from the inlet region model, $\varepsilon_\infty(R)$ is the fully developed turbulent viscosity profile, to be presented in the following, and λ is an empirical constant, determined in Cebeci and Chang (1978) through the adjustment of the centerline velocity numerical results to the experimental results of Dean (1972). The proposed value in Cebeci and Chang (1978) is $\lambda = 20$, obtained from the matching of results for $Re = 5 \times 10^4$. The same value of λ was employed here for comparison purposes.

Fully developed region ($Z > Z_H$)

The Nikuradse's relation for the mixing length is employed in this region, yielding the following working relation for the dimensionless turbulent diffusivity:

$$\epsilon_\infty = Re\left\{(0.14 - 0.08R^2 - 0{,}06R^4)\left[1-\exp\left[\frac{(R-1)}{26}\sqrt{-ReC}\right]\right]\right\}^2 \cdot \left|\frac{dU_\infty}{dR}\right| \tag{A7}$$

where,

$$C = \frac{dU_\infty}{dR} \tag{A8}$$

Appendix 2. Fully developed velocity profile

In the fully developed flow region, the governing equations reduce to:

$$\frac{1}{Re}\cdot\frac{d}{dR}\left[(1+\epsilon_{\infty}(R))\frac{dU_{\infty}}{dR}\right]-\frac{dp^{*}_{\infty}}{dZ}=0 \tag{A9}$$

where $\epsilon_{\infty}(R)$ and dp^{*}_{∞}/dZ are, respectively, the fully developed dimensionless turbulent diffusivity and axial pressure gradient, and the required boundary conditions are given by

$$\left.\frac{dU_{\infty}}{dR}\right|_{R=0}=0; \qquad U_{\infty}(1)=0 \tag{A10,11}$$

The turbulent viscosity, defined by equation (A7), may be written in the convenient form

$$\epsilon_{\infty}(R)=G(R)\left|\frac{dU_{\infty}}{dR}\right| \tag{A12}$$

where,

$$G(R)=Re\left\{F(R)\left[1-\exp\left(\frac{(R-1)}{26}\sqrt{-ReC}\right)\right]\right\}^{2} \tag{A13}$$

and,

$$F(R)=0.14-0.08R^{2}-0.06\,R^{4} \tag{A14}$$

The pressure gradient is determined from integration of equation (A9) over the channel cross-section, to yield:

$$\frac{dp^{*}_{\infty}}{dZ}=\frac{C}{Re} \tag{A15}$$

Integration of equation (A9) first yields the velocity gradient:

$$\frac{dU_{\infty}}{dR}=\frac{2CR}{1+\sqrt{1-4G(R)CR}} \tag{A16}$$

and a second integration from the channel wall to R, provides

$$U_{\infty}R=\int_{1}^{R}\frac{2CR'}{(1+\sqrt{1-4G(R')CR'}}dR' \tag{A17}$$

Finally, the velocity gradient at the duct wall is determined from satisfaction of the continuity equation

$$\int_{0}^{1}U_{\infty}(R)dR=1 \tag{A18}$$

which results in the following transcendental equation

$$A_{ijk}=\frac{1}{N_{i}^{1/2}N_{j}^{1/2}N_{k}^{1/2}}\int_{0}^{1}\psi_{i}(R)\psi_{j}(R)\psi_{k}(R)dR \tag{A19}$$

that can be handled with readily available subroutines for automatic integration and solution of non-linear equations (IMSL Library, 1987).

This profile was compared against the three layers velocity expressions provided by Reynolds *et al.* (see Arpaci and Larsen, 1984) with very good agreement.